20-GHz High-Efficiency Power Amplifiers Using Monolithic Multi-Cell Permeable Base Transistors

ROBERT ACTIS, KIRBY B. NICHOLS, RICHARD W. CHICK, AND ROY A. MCMORRAN

LINCOLN LABORATORY
MASSACHUSETTS INSTITUTE OF TECHNOLOGY
LEXINGTON, MASSACHUSETTS 02173

ABSTRACT - The performance at 20 GHz of high-efficiency power amplifiers using a new class of GaAs permeable base transistors (PBTs) is described. These devices utilize chip-level power-combining of multi-cell 8-by-20-μm PBT active areas and have demonstrated an output power of 437 mW with a power-added efficiency of 35% in a connectorized microstrip amplifier. The power, efficiency, and gain performance of demonstration amplifiers using these new devices is described.

INTRODUCTION

The GaAs permeable base transistor (PBT), developed at Lincoln Laboratory, has demonstrated very promising performance as a high-efficiency power transistor for applications up through K-band frequencies [1]-[2]. Discrete devices with active areas of 8 by 20 μm and 8 by 40 μm have exhibited power-added-efficiencies of 66% and 41% at 1.3 and 20 GHz respectively [2]. Although the power-added efficiency of the discrete PBT at high microwave and millimeter-wave frequencies has been exceptional to date, the output power capability of the device has been insufficient to overcome the high degree of circuit-combining required for many high-power applications.

For over a year now, a development effort has been underway to increase the power capability of the PBT and retain its high-efficiency performance for 20-GHz transmitter applications. The work has focused on the development of a device which utilizes chip-level power combining of several active-area PBT cells to increase the output power of the overall device.

Several in a series of new multi-cell PBT device wafers have been fabricated and evaluated. The devices on these initial wafers are comprised of dual-cell and four-cell 8-by-20-μm active area PBTs that are power-combined on a monolithic GaAs substrate. The resulting multi-cell devices represent a new class of PBTs that are well-suited to monolithic microwave integrated circuit (MMIC) applications and have significantly improved output power and high power-added efficiency.

In this paper, we describe the performance of power amplifiers which incorporate multi-cell PBT devices in microstrip circuit environments. Two multi-cell PBT structures, a dual-cell 250-mW device and a four-cell 400 mW device are used to demonstrate the improved power capability of amplifiers using these new PBT devices. The dc and small-signal RF characteristics and the large-signal load-pull performance of these PBTs at 20 GHz are described. In addition, the output power, gain, and associated power-added efficiency of microwave integrated circuit (MIC) amplifiers using these devices are also discussed. The combination of output power and associated power-added efficiency performance of these devices is the best reported for GaAs PBT amplifiers to date.

DESCRIPTION OF MONOLITHIC MULTI-CELL PBTS

The PBT is a vertical transistor in which the emitter and collector of the device are separated by a submicrometer-periodicity tungsten grating that forms the base of the transistor [3]. The tungsten grating is embedded in crystalline GaAs using an organometallic chemical vapor deposition overgrowth process. For each active area, two large tungsten base pads provide connection to the base gratings and are positioned such that a base pad

IF1

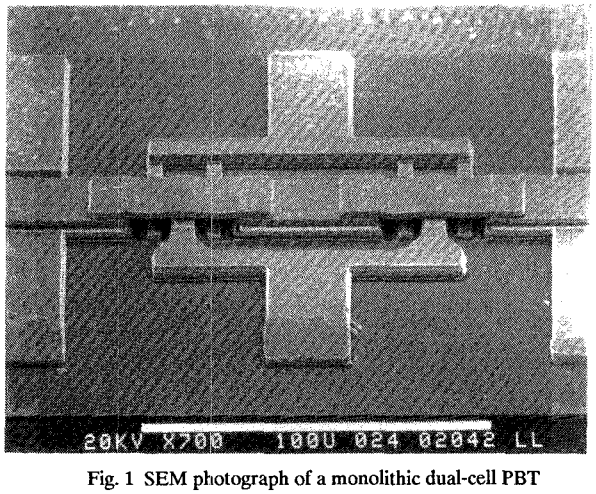

Fig. 1 SEM photograph of a monolithic dual-cell PBT

CH3141-9/92/0000-0281$01.00 © 1992 IEEE

rests on each side of the collector. Top-surface ohmic-contact metals are used to form the collector and emitter contacts. The emitter contact pads lie alongside the base pads on the top surface.

The multi-cell PBT structures described in this paper are based primarily on a dual-cell structure fabricated on a semi-insulating GaAs substrate. Air-bridge technology is used to interconnect the emitters from adjacent devices to ground [4]. A scanning electron microscope (SEM) photograph of the structure is shown in Fig. 1. Proton bombardment is used to define the 8-by-20-μm active areas and to provide device-to-device isolation. The device substrates are thinned to a 50-μm thickness to minimize thermal resistance and inductance to ground. The top-side base, collector, and emitter contacts of the devices enable each dual-cell device to be RF wafer probed. The smallest separation distance between active areas is 44 μm, which was determined to be sufficient to prevent the heating of an active area by adjacent active areas.

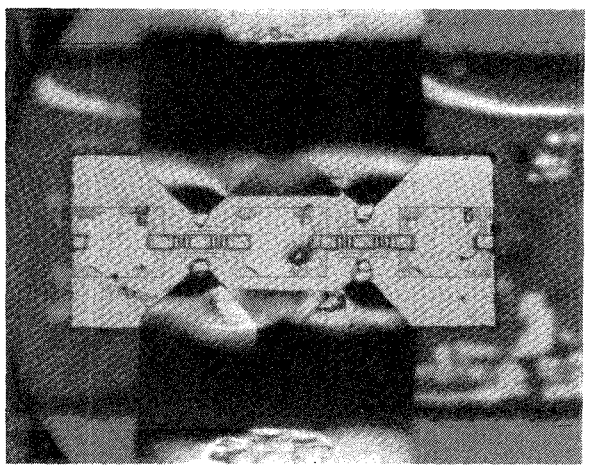

Fig. 2 Four-cell PBT bonded to an MIC substrate using photolithographicly fabricated ribbons. Via holes located between every dual-cell device provide the ground return.

The four-cell PBT is comprised of the parallel combination of two dual-cell devices with a center ground return located between each adjacent dual-cell structure. This configuration minimizes the equivalent transmission-line length between the active area and ground for the innermost devices and results in significantly improved gain and power-added efficiency than that provided by configurations that rely exclusively on air-bridges for the RF ground return. A four-cell PBT packaged into a 50-ohm microstrip transmission-line is shown in Fig. 2. The base and collector contacts are connected to the microstrip circuit using a photolithographically fabricated bonding ribbon

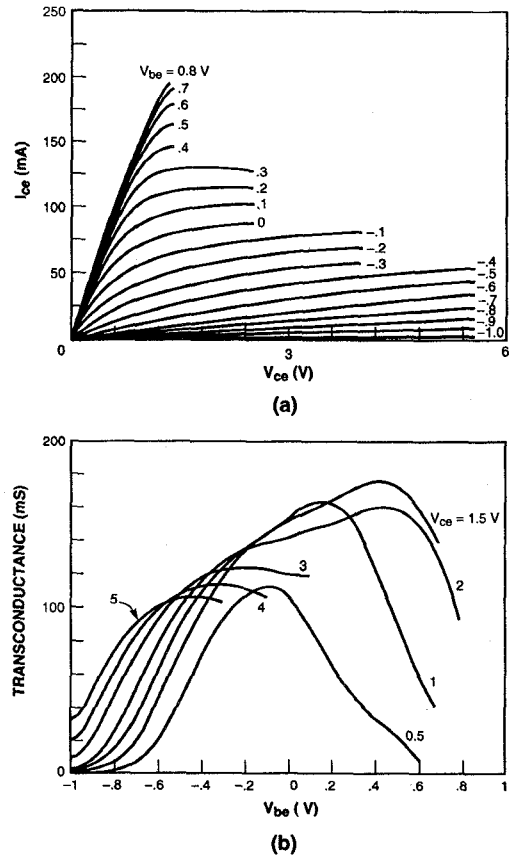

Fig. 3 (a) Collector current versus collector-emitter voltage for a dual-cell PBT. (b) Transconductance versus base-emitter voltage for a dual-cell PBT.

attached with thermocompression bonds. The four-cell PBT in this configuration results in low radiative losses and maintains high gain and power-added efficiency.

DC AND SMALL-SIGNAL CHARACTERIZATION

The current-voltage and transconductance g_m curves for a dual-cell PBT are shown in Fig. 3. The g_m for the dual-cell devices was nominally 85 to 95 mS measured at 50% of the zero-bias saturation current I_{ces}. The nominal value of I_{ces} was 90 mA. Figure 4 illustrates the small-signal transducer gain S_{21}, the maximum stable gain (MSG), and the current gain h_{21} for the dual-cell PBT. The data was obtained from on-wafer RF measurements.

The small-signal gain of the dual-cell device was nearly identical to that measured for single-cell PBTs from the same wafer. Other parameters of the device scaled as expected with the number of active cells, n (i.e., the device impedance scaled as 1/n, and I_{ces} and g_m scaled directly with n). The nominal unity current gain frequency f_T for dual-cell devices was extrapolated to 36 GHz. An MSG of

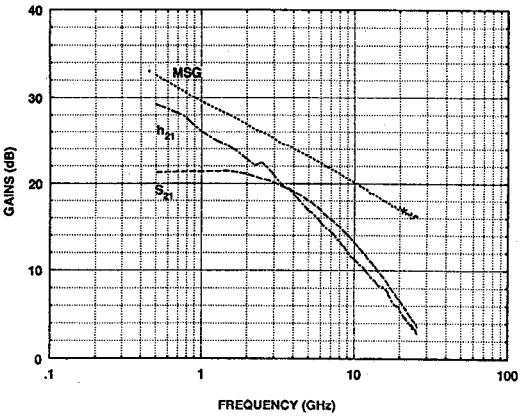

Fig. 4 Small-signal maximum stable gain (MSG), unity current gain h_{21}, and transducer gain as a function of frequency for dual-cell PBTs.

17 dB for single-cell PBTs and 16.3 dB for dual-cell devices was measured at 21 GHz.

The input and output impedances for these devices were sufficiently high to enable convenient microstrip impedance-matching techniques to be used in the amplifier design. The devices exhibited very unilateral small-signal characteristics with a reverse isolation S_{12} less than -25 dB at 20 GHz.

POWER CHARACTERIZATION

The large-signal characterization of the multi-cell PBTs at 20 GHz was performed using a computer-aided active load-pull measurement system [5]. The system was enhanced with an error-corrected power measurement technique similar to that described in Ref. 6. For these load-pull measurements, the devices were individually separated from the wafer and mounted into 0.010-in.-thick alumina microstrip circuits. The connection of the dual-cell device to the microstrip circuit was provided by 0.2-mil-thick photolithographically produced bonding ribbons. These interconnect ribbons were tapered on one end to facilitate thermocompression bonding to the 1.5-mil-square device contact pad. The opposing end of the interconnect ribbon was widened for convenient connection to 50-ohm microstrip transmission lines on alumina substrate. The use of photolithographically fabricated bond ribbons greatly improved packaging repeatability and minimized bonding inductances.

The load-pull measurements were carried out in the 19.7-to-21.7-GHz frequency band using a systematic search for the combination of device bias, drive power, and load impedance that delivered the optimum power-added efficiency. The measurement-system software provided direct control of these parameters with real-time display of device efficiency, output power, and embedding impedances.

Table I summarizes the best and typical measured load-pull results for the dual-cell and four-cell PBTs from two wafers. The dual-cell device easily demonstrated ¼-watt capability, while the four-cell device provided a nominal output power of 400 mW. In some cases, the results were obtained using input prematching circuits in order to minimize the error sensitivity associated with high reflection coefficient magnitudes. In addition, this served to maximize the incident power from sources with limited output power capability. The results tabulated in Table I include the circuit losses due to any pre-matching circuits.

Table I
20 GHz Load-pull Results for Dual-cell and Four-cell PBTs

Wafer	Device Type	Case	Gain (dB)	Output Power (mW)	Power-Added Efficiency	DC Power (mW)
2BB58	Dual-cell	best	5.3	334	44	532
2BB69	Dual-cell	typ.	5.9	246	40	457
2BB69	Four-cell	best	6.2	653	42	1,200
2BB69	Four-cell	typ.	5.3	436	35	960

Table II
Connectorized Multi-cell PBT Amplifier Performance at 20 GHz

Dual-cell Devices Used	Four-cell Devices Used	Gain (dB)	Output Power (mW)	Power-Added Efficiency	DC Power (W)
0	3	9.6	724	26%	2.49
1	1	9.5	417	31%	1.23
0	1	5.57	437	35%	0.89
0	2	4.44	700	26%	1.696
1	0	5.79	240	37%	0.47

AMPLIFIER DESCRIPTION AND PERFORMANCE

Using load-pull characterization, the optimum input and output embedding impedances for the dual-cell and four-cell PBTs were determined for a specific input drive and device bias at several discrete frequencies. The impedance-matching circuit designs were carried out with the assistance of commercially available computer-aided microwave circuit design software. The four-cell PBTs required impedance transformations to resistances of 3-5 ohms for the input circuit and 70 ohms for the output load. These impedance levels were one-half those required for the dual-cell devices. All the impedance-matching networks were realized using 0.010-in.-thick alumina microstrip. Table II summarizes the typical performance of connectorized PBT amplifiers using multi-cell PBTs inclusive of all circuit and connector losses.

Figure 5 illustrates the output power, gain, and power-added efficiency at 20 GHz of a two-stage microstrip PBT amplifier. The data is referred to the microstrip ports of the amplifier. The demonstration amplifier contains three four-cell devices with two devices combined using in-phase combiner/divider networks in the second stage of the amplifier. A four-cell device functions as the driver stage and is dc-isolated from the second stage by a coupled-line dc-blocking capacitor. Low-frequency oscillation-suppression networks fabricated with thin-film resistors and beam-lead capacitors were included at the input and output of each device to eliminate undesired instabilities at lower microwave frequencies. This amplifier has demonstrated an output power of 700 mW with a power-added efficiency of 26.5% and gain of 9.6 dB at 20 GHz. A photograph of the amplifier is shown in Fig. 6.

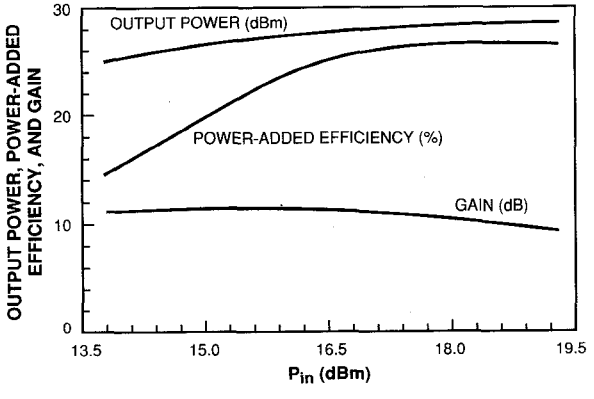

Fig. 5 Output power, gain, and power-added efficiency at 20 GHz for a 2-stage microstrip amplifier using four-cell PBTs. The data is referred to the microstrip ports.

SUMMARY

The performance of amplifiers incorporating a new class of GaAs PBTs have been described. These devices utilize chip-level power combining of 8-by-20-μm active area PBTs on a monolithic GaAs substrate. Two-cell (250 mW) and four-cell (400 mW) devices have been fabricated and embedded into 20-GHz high-efficiency MIC amplifiers which have demonstrated the high output power and power-added efficiency available from these PBTs.

ACKNOWLEDGEMENTS

The authors are grateful to and would like to acknowledge the contributions of many individuals that have made this work possible: R. G. Drangmeister for mask design, circuit/device packaging, and RF measurements, B. F. Gramstorff and D. J. Baker for wafer fabrication, and D. J. Landers for device packaging and MIC assembly. Additional assistance was provided by A. Vera, C. L. Dennis, B. J. Clifton, S. Rabe, H.H. Pichler, N. J. Bergeron, P.J. Daniels, L. J. Mahoney, D. A. Dedek, K. M. Molvar, M.D. McAleese, J. D. Woodhouse, J. M. Will, L. Cociani, N. Usiak, R. H. Mathews, G. L. Willman, L. P. Tedstone, J. S. Taibbi, and D. M. Klays. The authors would also like to thank L. J. Kushner for many helpful discussions, A. D. Barlas for his indispensable assistance in addressing reproducibility in PBT fabrication, T. E. Kazior from the Raytheon Research Division for assistance in via-hole fabrication, and R. A. Murphy, M. A. Hollis, and D. R. McElroy for their support and encouragement.

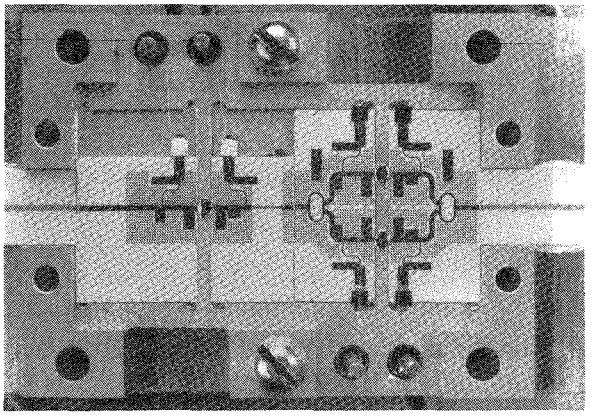

Fig. 6 Demonstration two-stage PBT amplifier

REFERENCES

1. L. J. Kushner, M. A. Hollis, R. H. Mathews, K. B. Nichols, and C. O. Bozler, "22 GHz Performance of the Permeable Base Transistor," *Digest of Technical Papers, IEEE MTT International Microwave Symposium*, New York, NY, 1988, pp. 525-528.

2. K. B. Nichols, M. A. Hollis, C. O. Bozler, M. A. Quddus, L. J. Kushner, R. H. Mathews, A. Vera, S. Rabe, R. A. Murphy, and D. L. Olsson, "High Power-Added Efficiency Measured at 1.3 and 20 GHz Using a GaAs Permeable Base Transistor," *Proc. IEEE/Cornell Conf. on Adv. Concepts in High Speed Semicond. Devices and Circuits*, Cornell Univ., Ithica, NY, p. 307 (1987).

3. Sze, *et al.*, "Physics of Semiconductor Devices", Chapter 4, Homogeneous Field-Effect Transistors, M. A. Hollis and R. A. Murphy.

4. K. B. Nichols, R. Actis, C. L. Dennis, A. D. Barlas, D. J. Baker, B. F. Gramstorff, R. G. Drangmeister, A. Vera, and R. W. Chick, "20 GHz Performance of Multi-Cell Power Permeable Base Transistors Fabricated Using Scanning Electron Beam Lithography," To be published.

5. R. Actis and R. A. McMorran, "Millimeter Load Pull Measurements," *Applied Microwave Magazine*, Nov./Dec. 1989, pp. 91-102.

6. R. S. Tucker and P. D. Bradley, "Computer-Aided Error Correction of Large-Signal Load-Pull Measurements," IEEE Trans MTT, 1984, pp. 296-300.

This work was supported by the Defense Advanced Research Projects Agency and the Departments of the Army and Air Force.